

https://doi.org/10.1070/QEL16958

Analysis of spectroscopic information for detecting methane emissions on local paths using CO and He–Ne lasers

O.K. Voitsekhovskaya, D.E. Kashirskii, O.V. Shefer

Abstract. **Measuring the concentration of methane in the atmosphere is demonstrated to be very important, since an increase in methane content enhances the greenhouse effect. It is shown that the error in assessing the concentration of CH_4 depends on many factors, including the reliability of the parameters of the spectral absorption lines of gases, the accuracy of determining the concentration, the measurement error, etc. The spectroscopic information necessary to detect sources of high methane concentration in the atmosphere using CO and He–Ne lasers is analysed.**

Keywords: *laser, methane, concentration, absorption spectrum, differential absorption method.*

1. Introduction

Intensive emission of methane from natural (swamps, ponds, geochemical processes) and anthropogenic (coal mines, gas pipelines, combustion processes) sources increases its concentration in the Earth's atmosphere. One of these sources is presented by gas hydrates, or clathrates, which are crystalline compounds formed at high pressure and low temperature from water and gas. Under the bottom of the Arctic Ocean methane hydrates are accumulated containing about 160–180 volumes of methane in one volume. The greatest interest of researchers is attracted by the destruction of methane gas hydrates as a result of a rise in the level of the World Ocean and an increase in the water temperature of the shelf arctic seas [1–3].

From an applied point of view, the detection of gas hydrates and bubbles with high concentration of methane can serve as an indicator of the presence of oil and gas deposits and fault zones. However, the greatest attention is paid to the danger of involving bottom methane deposits in the biogeochemical cycle of the Earth's atmosphere. A joint assessment of the microphysical characteristics of methane in a gaseous or solid state in aqueous or above-water environment relies on the results of the study of methane hydrates by optical methods [4, 5], including laser sensing [6]. High sensitivity in determining the parameters of a medium containing methane is achieved by absorption spectroscopy in the middle and near-IR ranges, where active vibrational–rotational absorption bands of methane are located.

Currently, many scientific teams carry out the monitoring of the methane content in the Earth's atmosphere in the near- and middle-IR regions. Most instruments for methane monitoring use the differential absorption method (DAM) [7] at various wavelengths. The basic principle of DAM is to measure the absorption coefficients of a probed gaseous compound using two laser lines, chosen so that the absorption is maximal for one line and minimal for the other one. Determining the difference of these values allows the absorption coefficient (AC) of the probed gas to be found, because the effect of background absorption is suppressed.

Long-term measurements of the methane content on the Earth's surface on land and at sea are carried out [8, 9]. Observations from satellites make it possible to determine the methane content in the entire atmosphere, which, in combination with modelling, expands knowledge about methane sources for predicting climatic conditions on Earth. Valuable information comes from the satellite spectrometer SCIAMACHY (Scanning Imaging Absorption Spectrometer for Atmospheric Chartography), based on the ENVISAT satellite of the European Space Agency [10–12]. We would also like to mention the satellite system bearing the MIPAS (Michelson Interferometer for Passive Atmospheric Sounding). With its help, many atmospheric and impurity gases, including methane, are monitored [13].

The Raman scattering method is also used [14], the advantage of which is the possibility of recording a vertical methane profile, which was carried out up to an altitude of 4 km with a step of 100 m using a three-frequency Nd:YAG laser. The agreement between the measured rate of photocounts in the Raman CH_4 channel in the free troposphere and the rate obtained by numerical simulation for a typical background concentration (2 ppm) of CH_4 confirms the reliability of determining the CH_4 content.

In recent years, special attention was paid to the study of methane spectra in the near-IR region, which is motivated by satellite measurements of the thermal radiation spectra of the Earth and its atmosphere. When sensing from space, vertical paths are most widely used. In this case, the methane absorption band at $\lambda = 3.39$ μm is not suitable for sensing, because the entire atmosphere appears to be completely opaque at this wavelength. Therefore, for satellite measurements, methane absorption bands at wavelengths of 0.76, 1.6, and 2.0 μm are used, where the absolute methane absorption coefficient is much smaller. Lidars are used using optical parametric ampli-

O.K. Voitsekhovskaya, D.E. Kashirskii Tomsk State University, prosp. Lenina 36, 634050 Tomsk, Russia; e-mail: kde@mail.tsu.ru;
O.V. Shefer Tomsk Polytechnic University, prosp. Lenina 30, 634050 Tomsk, Russia

Received 1 February 2019; revision received 6 March 2019
Kvantovaya Elektronika **49** (9) 881–886 (2019)
Translated by V.L. Derbov

fiers and oscillators (OPOs). Modified after passing through the atmosphere, the OPO radiation is detected by an avalanche photodetector [15, 16].

However, errors in connecting to exact geodetic coordinates leave relevant the measurements of atmospheric transparency on limited paths using ship-based or car-based mobile systems [17]. Such a measurement scheme was implemented at the Norwegian Institute for Air Research [18], involving not only ship-based, but also airborne instruments. Similar work is carried out by other researchers [19, 20]. In the case of short (about 20 m) ground paths, it is undoubtedly preferable to use the methane absorption band at $\lambda = 3.39$ μm, because according to our calculations, the absolute AC value in the spectral region 3.22–3.31 μm (3105–3020 cm^{-1}) is 35–40 cm^{-1} atm^{-1}, while the maximum AC of methane in the band 1.6 μm within the spectral region 1.639–1.652 μm (6100–6050 cm^{-1}) is only 0.4 cm^{-1} atm^{-1}.

Great fame was gained by the MERLIN (Methane Remote Lidar Sensing Mission) project [21], proposed by French and German researchers to control the methane content from a satellite. The authors of the project paid most attention to achieving maximum accuracy in determining the concentration of methane in the column of the Earth's atmosphere. The purpose of the MERLIN mission is to measure the spatial and temporal gradients of atmospheric CH_4 with high accuracy. As the main result, the ratio of concentrations in the mixture of dry air and CH_4 is to be extracted from the MERLIN data. For this aim, the DAM principle is implemented, i.e., measuring the difference in atmospheric transmittance for laser radiation with a wavelength located in the centre or near the centre of the CH_4 absorption line ($\lambda_{on} = 1.64555$ μm) and radiation with a reference wavelength ($\lambda_{off} = 1.64585$ μm) with significantly lower absorption. The receiving system collects backscattered photons and focuses them on the detector. Since the backscattered signals are very weak, it is necessary to accumulate several separate signals along the path in order to reach the threshold level of the photodetector sensitivity.

In this paper, we analyse the use of lasers generating electromagnetic radiation in the spectral region of maximum absorption by methane to determine the methane concentration on local paths.

In this case, the accuracy of the absolute AC values used in solving the inverse problem is particularly important for finding the methane concentration. A number of calculations are based on the data obtained by studying absorption in cells with a reference gas content, while others are based on theoretical concentration dependences of AC or transmission functions (TF). When constructing the concentration dependence of the AC or TF, errors are inevitable due to those in both the experiment and the theory of deriving the AC and TF from the parameters of spectral lines.

2. Methods

The method for calculating atmospheric transparency is standard [22]. The calculation of the transmission spectrum of an inhomogeneous gas–aerosol medium is based on the idea of dividing it into homogeneous layers, in which local thermodynamic equilibrium exists. The real spectrum is calculated as a convolution of a high-resolution spectrum with the instrument function of the receiver. The transmission function of such a gaseous medium at a frequency ν_0 is described by the formula:

$$\tau(\nu_0) = \int\prod_M \tau_m(\nu_0) A(\nu_0, \nu)\,\mathrm{d}\nu,$$

where

$$\tau_m(\nu_0) = \exp\left[-\sum_i k^i_{\mathrm{sel}}(\nu_0, T_m, p_m)\rho_{mi} l\right]$$

is the transmission function of the mth layer; M is the number of layers; and $A(\nu_0, \nu)$ is the instrument function of the receiver. According to the line-by-line method, the absorption coefficient of the ith gas in the mth layer $k^i_{\mathrm{sel}}(\nu_0, T_m, p_m)$ is obtained by summing the contributions of the absorption spectral lines of the gas component to the absorption at the frequency ν_0:

$$k^i_{\mathrm{sel}}(\nu_0, T_m, p_m) = \sum_j S_{ij}(\nu_{ij}, T_m, p_m) f(\nu_0, \nu_{ij}, T_m, p_m),$$

where $S_{ij}(\nu_{ij}, T_m, p_m)$ is the intensity of the jth absorption line of the ith gas component; $f_{ij}(\nu_0, \nu_{ij}, T_m, p_m)$ is the contour of the absorption line; T_m is the temperature of the layer; p_m is the total pressure in the layer; l is the optical path length; and ρ_{mi} is the partial pressure of the ith gas component in the mth layer. From this technique, it follows that the accuracy of the result is determined by the accuracy of the spectral line parameters (SLPs).

A number of spectroscopists are working to improve the accuracy of methane SLPs [23–25]. The methane molecule is a T_d symmetry tetrahedron, the main moments of its inertia are equal to each other, and therefore, CH_4 belongs to spherical tops. The high symmetry of this molecule leads to the fact that only two out of nine possible fundamental vibrations give rise to active vibrational–rotational bands in the IR spectrum, corresponding to triply degenerate vibrations ν_3 (3.31 μm) and ν_4 (7.65 μm). Practical problems associated with the molecule led to considerable interest in it among researchers and initiated a wide discussion of the spectral characteristics of CH_4 in the world literature [26].

This paper analyses the reliability of spectroscopic information used to determine the methane concentration on various paths from atmospheric transparency measurements. The wavelength region near 3 μm is considered, since the most intense absorption by CH_4 is observed in this region. Calculations were performed using the HITRAN2016 database (DB) [23], in which the data on the spectral absorption lines of methane were changed as compared to the previous data [24]. Thus, in the region of 9–1370 cm^{-1}, many hot bands were removed, because their intensities in the HITRAN2012 database were overestimated by orders of magnitude. In the range 1370–4000 cm^{-1}, the centres of methane absorption lines were refined, while the intensities and half-widths were borrowed from the previous version. The HITRAN database includes SLPs of various isotopes of gases, but in this paper, we consider only the main isotopes of gases that make up the atmosphere.

3. Results

3.1. Absorption coefficient of He–Ne-laser radiation by methane

The authors of Refs [27, 28] present the measured methane absorption coefficients for the lines of He–Ne-laser radiation with $\lambda_1 = 3391.2$ nm (2948.8087 cm^{-1}) and $\lambda_2 = 3392.2$ nm

(2947.9394 cm^{-1}). In Ref. [28], to assess the sensitivity of the developed laser system, the authors measured the attenuation of radiation at both wavelengths in a 1-m-long cell at a methane concentration of 110 ppm. Methane absorption at λ_1 was not recorded and at λ_2 it was 0.05. The use of a multipass cell under field conditions made it possible to increase the optical path to 20 m, and the absorption at λ_2 amounted to 0.05 for the path length 7.2 m at a CH_4 concentration of about 15 ppm. The authors of [28] noted the presence of fluctuations in the characteristics of the emission lines of the He–Ne laser in the course of oscillations. Their origin is considered in detail in Ref. [29]. Specific features of a particular laser system (its external and internal parameters) lead to a change in the real radiation frequency in a certain range individual for each laser. Consequently, the value of the measured gas absorption coefficient varies within this interval. The half-width of the spectrum of one laser mode is determined by the length of the laser cavity and the partial loss of radiation during its propagation inside the cavity. In Ref. [29], the half-width of the laser line was calculated, which amounted to 0.00069 cm^{-1}. When processing the experimental data, it was assumed that the laser operation is single-mode with $\lambda_2 = 3392.235$ nm.

We calculated the absorption coefficients using the program [30] with the following input data: the spectral wavenumber step is 0.01 cm^{-1}, the gas temperature is 296 K, the emission line contour is triangular, and the CH_4 absorption line has the Voigt contour. We should especially dwell on the choice of the emission line width, since the data on it for the He–Ne laser with $\lambda = 632.8$ nm taken from different sources vary from 0.01 cm^{-1} [26] to 0.03–0.05 cm^{-1} [29]. The width of the gain band (emission line) at the transition with $\lambda = 632.8$ nm of the He–Ne laser is determined by the Doppler effect. It is difficult to calculate this value accurately for the 3.39 μm band using the formulae of Ref. [31] because the mixture consists of two gases with different molecular weights and unknown concentration ratio, and the cavity mode width, active medium temperature, and pump level are unknown. Therefore, the value of 0.01 cm^{-1} was chosen for the calculations according to the data of Ref. [27].

In the literature, not only different values of the He–Ne-laser line widths are presented, but also different values of their wavelengths. Thus, in Ref. [27], the value $\lambda_2 = 3392.235$ nm (2947.909 cm^{-1}) was obtained, and in Ref. [28], $\lambda_2 = 3392.2$ nm (2947.9394 cm^{-1}). Similarly, for λ_1, the value of 3391.2 nm (2948.8087 cm^{-1}) was indicated in Ref. [28], and 3391.3 nm (2948.7217 cm^{-1}) in Ref. [32].

The calculation for the working conditions [28] showed that methane absorption at $\lambda_1 = 3391.2$ nm and $\lambda_2 = 3392.2$ nm is absent, and at $\lambda = 3392.211$ nm (2947.930 cm^{-1}) a 5% absorption corresponding to the experimentally measured one is detected. Simulation for field conditions of measurements also gave an absorption coefficient of 5% at a methane concentration of 10 ppm, in contrast to the concentration of 15 ppm indicated in [28].

The simulation of methane absorption coefficients measured in Ref. [27] at the emission lines of the He–Ne laser led to the following results. As follows from [27], the experimental value of the methane AC at $\nu_2 = 2947.909$ cm^{-1} is 8.55 cm^{-1} atm^{-1}. The calculation gives an AC value of 8.83 cm^{-1} atm^{-1}, which coincides with the experimental value within the experimental error. For $\nu_1 = 2948.808$ cm^{-1}, the calculation yields an AC value of 0.89 cm^{-1} atm^{-1}; for $\nu_1 = 2948.7217$ cm^{-1} the AC is 0.53 cm^{-1} atm^{-1}.

It follows from the review part of Ref. [29] that the position of the centre of the laser line $\nu_2 = 2947.909$ cm^{-1} is reliable up to the fourth decimal place, but the SLP values of the methane absorption line closest to ν_2 are determined with a larger error. Thus, according to Ref. [23], its intensity is 1.25 cm^{-1} atm^{-1}, and in Ref. [29] the value of 1.36 ± 0.06 cm^{-1} atm^{-1} is given, which is beyond the error limits. Note that the experimental AC value reported in Ref. [29] is 8.7 ± 0.36 cm^{-1} atm^{-1}, which practically coincides with our calculated value of 8.83 cm^{-1} atm^{-1}. This evidences in favour of the reliability of the used value of the line half-width.

Such a detailed discussion is aimed to understand the accuracy required from SLPs and other input data to model the process of radiation propagation in a gaseous medium. After such a consideration, it would be more acceptable to use reference AC measurements in cells with a known amount of the tested gas; however, in this case, errors in determining gas concentrations in the reference mixture are also possible because of their actual purity, temperature measurement error, etc.

3.2. Methane AC at the wavelengths of CO laser lines

To clarify the AC values of the CH_4 used in the differential absorption method [33], we also calculated the methane AC at the wavelengths of the CO laser oscillation (Table 1). The initial data for the calculation are as follows: the emission line contour is Gaussian, the line width is 0.001 cm^{-1}, and the spectral step is 0.001 cm^{-1}. The rest of the input data are the same as in Section 3.1. Table 1 also presents the wavenumber intervals, for which the AC value is valid taking into account the measurement error, as well as the wavenumber values, for which the calculated AC, k_{cal}, coincides with the measured one, k_{exp}.

In Ref. [33], the AC values were measured with a very large error and cannot serve as a criterion for checking the reliability of methane SLP values. However, worth attention is the discrepancy between the calculated and experimental results for the line 3006.95 cm^{-1}, which exceeds 50%. Therefore, it is necessary to evaluate additionally the parameters of methane absorption lines in the region of 3 μm.

As already mentioned, the data on absorption SLPs (centres, intensities, half-widths, quantum identification of spectral lines) for this gas are collected in well-known databases such as HITRAN and GEISA [23–25], with extensive references. These SLP bases are compilation sets of parameters for methane absorption lines. We also note the original databases [34–36]. However, comparing the data of these sources with each other is difficult for a number of reasons, the discussion of which can be found, e.g., in Ref. [37]. Nevertheless, the importance of the reliability of the information provided is difficult to overestimate, since SLP values are the basis for the implementation of practical tasks.

We found in the literature two sets of experimental Fourier absorption spectra of methane in the IR region. The first one is the results of measurements in the Pacific Northwest National Laboratory (PNNL), USA, [38] at a gas temperature of 298 K. The measurements were carried out in PNNL under the following conditions: the average spectral resolution was 0.1 cm^{-1}, the step varied from 0.015 to 0.06 cm^{-1}. The website [39] contains text files with methane AC values in ppm^{-1} m^{-1} and a factor of 23025.9 to convert them into the units cm^{-1} atm^{-1}, which we also used.

Table 1. Characteristics of methane absorption of radiation at CO-laser oscillation lines.

Identification of laser transition	Frequency of laser line centre/cm^{-1}	k_{cal} /cm^{-1} atm^{-1}	$k_{exp} \pm \Delta$ /cm^{-1} atm^{-1} [33]	$\nu(k_{exp} - \Delta) - \nu(k_{exp} + \Delta)$ /cm^{-1}	$\nu(k_{cal} = k_{exp})$ /cm^{-1}
22 P8	3105.07	0.53	0.46±0.11	3105.05–3105.16	3105.107
22 P10	3097.75	0.046	0.064±0.03	3097.22–3097.34	3097.295
22 P11	3093.98	0.19	0.23±0.08	3094.015–3094.09	3097.75
23 P7	3059.46	0.08	0.10±0.04	3059.894–3060.25	3059.236
24 P6	3013.86	3.50	3.54±0.32	3013.850–3014.017	3013.86
24 P7	3010.44	0.63	0.75±0.22	3010.40–3010.61	3010.477
24 P8	3006.95	0.22	0.54±0.03	3007.353–3007.372	3007.365

The second data set, available at the website [40], was obtained at the Laboratory of Chemical Kinetics and Laser Sensors of King Abdullah University of Science and Technology in Saudi Arabia. In this laboratory the research on methane spectroscopy in a wide temperature range of 296–1120 K is carried out. The results of this research on the methane spectrum near 3 μm are published in Refs [27, 41]. We calculated the methane AC in accordance with the conditions for measuring this value at a spectral resolution of 0.01 cm^{-1} based on the HITRAN2016 database. The following parameters were used: the instrument function of the spectrometer was triangular, the spectral step was 0.1 cm^{-1}, and the gas temperature was 298 K. The triangular instrument function is convenient for accelerating the calculations, but its real shape for the Fourier spectrometer is more complicated [42]. Figure 1 shows two experimental methane absorption spectra and the one calculated by us. It is clearly seen that for the 24 P8 line (3006.95 cm^{-1}) the use of the data [23] cannot be recommended because of the significant discrepancy between the calculated and experimental values of the AC. Almost complete coincidence of the results of independent experiments allows us to conclude that the situation is somewhat similar to that with the absorption spectrum of water vapour [43], when against the general background of reliable data in the HITRAN database there are parts of the spectrum whose data do not correspond to the real SLP values. Thus, when choosing the operating laser radiation lines, a similar analysis should be conducted in advance, based on a comparison of the calculated and experimental AC values.

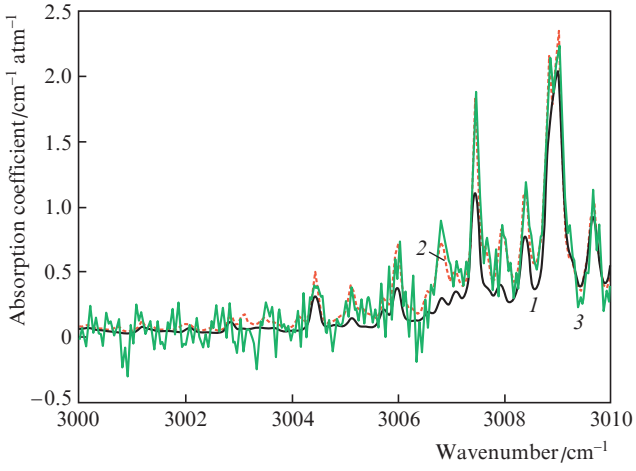

Figure 1. Methane absorption spectra calculated based on the HITRAN2016 database [23] (*1*) and measured in Refs [39] (*2*), [40] (*3*) in the spectral range 3000–3010 cm^{-1}.

Consider the spectral dependence of the methane AC in the mid-IR region (Fig. 2). Obviously, at low methane concentrations, the working parts of the spectrum should be the regions near the centre of the bands with maximum AC.

For a more detailed analysis of the spectral dependence at the band maxima, Fig. 3 shows the AC spectra calculated with the step and resolution of 0.01 cm^{-1} in the region 3016–3020 cm^{-1} of maximal absorption. To assess the reliability of the SLP data from the HITRAN2016 database in

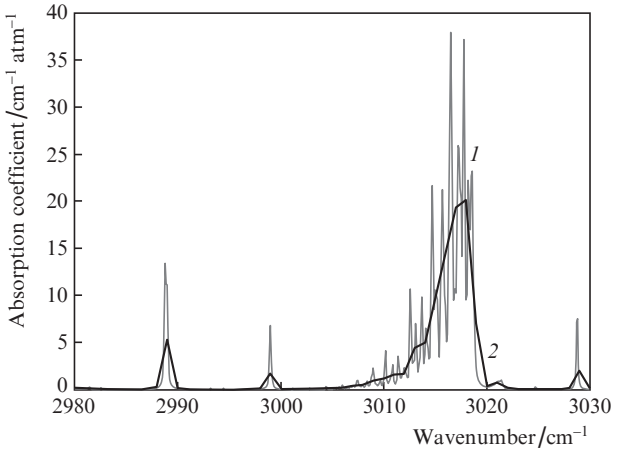

Figure 2. Dependences of the CH_4 absorption coefficient on the radiation wavenumber for the ν_3 band, calculated with the same step and spectral resolution of (*1*) 0.1 and (*2*) 1 cm^{-1}.

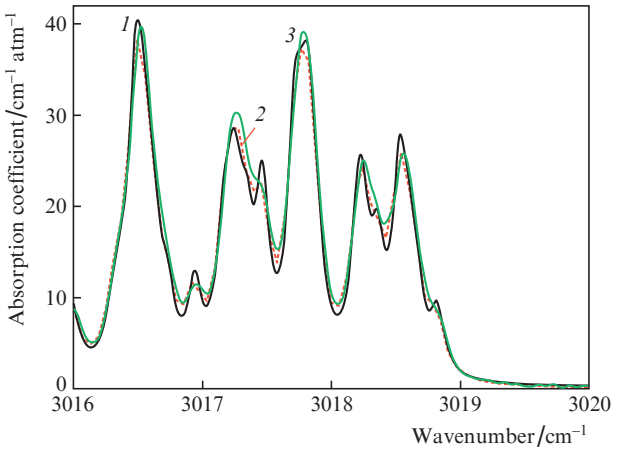

Figure 3. Methane absorption spectra calculated from the HITRAN2016 database [23] (*1*) and measured in Refs [39] (*2*), [40] (*3*) in the spectral range 3016–3020 cm^{-1}.

this spectral region, we compared these data with the experiment, as it was done for the region of 3000–3010 cm^{-1}. We note that the calculated and experimental data agree well enough; therefore, this is a suitable spectral range for choosing the laser emission lines for methane sensing. The most diverse spectrum of radiation at vibrational–rotational (VR) transitions is possessed by a CO laser.

We have proposed a method for refining the energies of highly excited quantum states of a CO molecule with rotational quantum numbers greater than 25 based on new values of the Dunham parameters [44] and, therefore, new values of the line centres of radiative transitions in the CO molecule. According to Ref. [45], in the CO laser the most intense radiation is observed at the VR transitions of the bands $V' = 25 \rightarrow V'' = 23$ and $V' = 26 \rightarrow V'' = 24$. Our calculations of the emission line centres in the CO laser and the methane AC show that among these bands, the following vibrational–rotational transitions appear to be most suitable for DAM measurements: for the first CO band, the 'on-line' line with ν = 3016.924 cm^{-1} ($J' = 17 \rightarrow J'' = 18$) and with the methane AC 12.52 cm^{-1} atm^{-1}, the 'off-line' line with ν = 3021.129 cm^{-1} ($J' = 16 \rightarrow J'' = 17$) and with the methane AC 0.082 cm^{-1} atm^{-1}; for the second CO band, the 'on-line' line with ν = 3017.2096 cm^{-1} ($J' = 4 \rightarrow J'' = 5$) and with the methane AC 26.98 cm^{-1} atm^{-1}, the 'off-line' line with ν = 3020.490 cm^{-1} ($J' = 3 \rightarrow J'' = 4$) and with the methane AC 0.379 cm^{-1} atm^{-1}. The first pair of lines is preferable, since the laser radiation power for these lines is much higher [45].

Unfortunately, it was not possible to select the emission line of the CO laser corresponding to the peak AC values of methane in this region, as noted earlier in the literature.

The use of DAM for laser monitoring of methane concentration is also discussed in Refs [46, 47], but the insufficient information about the conditions of the experiment did not allow us to reproduce the reported results. It was proposed to use an optical parametric oscillator as an alternative source [48]; but for this task its radiation linewidth is too large. However, for long paths (of the order of 2 km) this source is quite applicable.

It should be noted that the effect of the aerosol component of the atmosphere on the CH_4 sensing is usually not considered, since the DAM is based on two measurements of the AC ('on line' and 'off line'), and the contribution of the aerosol component to the difference $\tau_{on} - \tau_{off}$ can be neglected, because the spectrum of aerosol attenuation is usually sufficiently smooth. However, in some cases, when in the region of 3 μm the frequency dependence of the aerosol transmission function τ_{aer} has oscillations [49, 50], this effect should be taken into account. Particles comparable with the incident radiation wavelength, and large predominantly oriented plate crystals possess the most pronounced spectral dependence of the attenuation of optical radiation among all dispersed components [51]. In addition, the microphysical, optical and orientation properties of particles, as well as their chemical composition can significantly affect the nature of oscillations of attenuation of visible and IR radiation [52, 53].

We carried out a series of numerical experiments to determine the attenuation of optical radiation transmitted through a system of spherical particles. To calculate the integral attenuation characteristic, a modified gamma distribution was used. Figure 4 presents the dependences of the absorption coefficients k_{aer} and transmission functions τ_{aer} on λ calculated with complex refractive index $\tilde{n}(\lambda)$ for marine aerosol with different values of the mean radius $\bar{a}$ of the spheres,

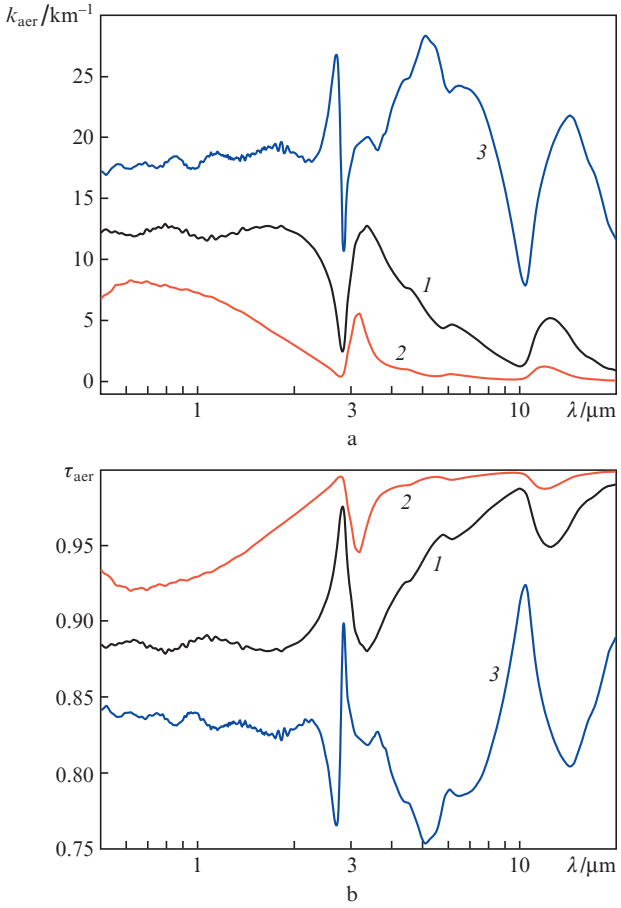

Figure 4. (a) Attenuation coefficients $k_{aer}(\lambda)$ and (b) transmission function $\tau_{aer}(\lambda)$ at l = 10 m and the following parameters: (*1*) $\bar{a}$ = 1 μm, $C = 10^6$ L^{-1}, μ = 1; (*2*) $\bar{a}$ = 1 μm, $C = 10^6$ L^{-1}, μ = 20; and (*3*) $\bar{a}$ = 5 μm, $C = 10^5$ L^{-1}, μ = 20.

parameter μ of the modified gamma size distribution of particles, and concentration of particle C.

From Fig. 4 it is seen that the advantage of DAM in some parts of the spectrum for a number of aerosol particles is devaluated. Thus, e. g., there is a sharp change in the transmission function with the variation of the wavelength in the region near 3 μm. Therefore, a rigorous analysis of the spatial and size distributions of aerosol particles, as well as taking into account the possible influence of these factors, is necessary even in the case of measurements on a local path.

4. Conclusions

The analysis of spectroscopic information for detecting methane emissions in the atmosphere using CO and He–Ne lasers is reported. We have shown that in the HITRAN database there are regions of the methane spectrum, in which the data do not correspond to the actual values of the spectral line parameters observed in the experiment. The ambiguity in the values of the centre frequencies and widths of the laser emission lines given in literature is revealed. It is demonstrated that in certain parts of the spectrum in the presence of certain types of aerosol particles, it is necessary to control the wavelength gradient of the transmission function, when using the differential absorption method. Thus, when choosing the working wavelengths of laser radiation to determine the methane concentration by the differential absorption method, it is nec-

essary to analyse the used spectroscopic information thoroughly.

Acknowledgements. This research was supported by the TSU Competitiveness Enhancement Program (Grant No. 8.2.04. 2018).

References

1. Yurganov L.N., Leifer A., Myhre Lund C. *Sovremennye Problemy Distantsionnogo Zondirovaniya Zemli iz Kosmosa*, **13** (2), 107 (2016).
2. Yurganov L.N., Leifer A. *Sovremennye Problemy Distantsionnogo Zondirovaniya Zemli iz Kosmosa*, **13** (3), 173 (2016).
3. Anisimov O.A., Kokorev V.A. *Izvestiya. Atmos. Ocean. Phys.*, **51** (9), 979 (2015) [*Issledovaniye Zemli iz Kosmosa*, No.2, 20 (2015)].
4. Parker R., Boesch H., Cogan A., et al. *Geophys. Res. Lett*., **38**, L15807 (2011).
5. Riris H., Numata K., Li S., et al. *Appl. Opt*., **51** (34), 8296 (2012).
6. Webster K.D., White J.R., Pratt L.M. *Arct. Antarct. Alp. Res*., **47** (4), 599 (2015).
7. Mezheris R. *Lazernoe distantsionnoe zondirovanie* (Laser Remote Sensing) (Moscow: Mir, 1987).
8. Myhre C.L., Ferré B., Platt S.M., et al. *Geophys. Res. Lett*., **43**, 4624 (2016).
9. https://www.esrl.noaa.gov/gmd/ccgg/data-products.html.
10. Frankenberg C., Meirink J.F., Bergamaschi P., et al. *J. Geophys. Res*., **111**, D07303 (2006).
11. Schneising O., Buchwitz M., Burrows J.P., et al. *Atmos. Chem. Phys*., **9**, 443 (2009).
12. Frankenberg C., Meirink J.F., van Weele M., et al. *Science*, **308**, 1010 (2005).
13. http://envisat.esa.int.
14. Veselovskii I., Goloub P., Hu Q., et al. *Atmos. Meas. Tech*., **12**, 119 (2019).
15. Riris H., Numata K., Wu S., et al. *J. Appl. Remote Sens*., **11**, 034001 (2017).
16. Refaat T.F., Ismail S., Nehrir A.R., et al. *Opt. Express*, **21**, 30415 (2013).
17. https://www.pergam.ru/articles/detektirovanie-utechek-gaza.htm.
18. http://ebas.nilu.no.
19. Kodovska F.G.-T., Sparrow K.J., Yvon-Lewis Sh.A., et al. *Earth Planet. Sci. Lett*., **436**, 43 (2016).
20. Nagornyi A.P., Makshtas A.P. *Problemy Arktiki i Antarktiki*, **87** (1), 22 (2011).
21. https://directory.eoportal.org/web/eoportal/satellite-missions/content/-/article/merlin.
22. Timofeev Yu.M., Vasiliev A.V. *Teoreticheskiye osnovy atmosfernoi optiki* (Theoretical Foundations of Atmospheric Optics) (St. Petersburg: Nauka, 2003).
23. Gordon I.E., Rothman L.S., Hill C., et al. *J. Quant. Spectrosc. Radiat. Transfer*, **203**, 3 (2017).
24. Rothman L.S., Gordon I.E., Babikov Y., et al. *J. Quant. Spectrosc. Radiat. Transfer*, **130**, 4 (2013).
25. Jacquinet-Husson N., Armante R., Scott N.A., et al. *J. Quant. Spectrosc. Radiat. Transfer*, **327**, 31 (2016).
26. Amyay B., Boudon V. *J. Quant. Spectrosc. Radiat. Transfer*, **219**, 85 (2018).
27. Alrefae M., Es-sebbar E., Farooq A. *J. Mol. Spectrosc*., **303**, 8 (2014).
28. Jordan K.J., Menzel E.R. *Proc. SPIE*, **737**, 80 (1987).
29. Mallard W.G., Gardiner W.C. Jr. *J. Quant. Spectrosc. Radiat. Transfer*, **20** (2), 135 (1978).
30. Voitsekhovskaya O.K., Voitsekhovskii A.V., Egorov O.V., et al. *Proc. SPIE*, **9292**, 929211 (2014).
31. Letuta S.N. *Metodicheskie ukazaniya k laboratornym rabotam po kursu 'Osnovy fiziki lazerov'* (Guidelines for Laboratory Work on the Course 'Fundamentals of Laser Physics') (Orenburg, Izd-vo OGU, 1999).
32. *Springer Handbook of Lasers and Optics. Part 11. Lasers and Coherent Light Sources* (Springer, 2007).
33. Persijn T., Santosa E., Harren F.J.M. *Appl. Phys. B*, **75**, 335 (2002).
34. http://vpl.astro.washington.edu/spectra/ch4nirimages.htm.
35. Yurchenko S.N., Amundsen D.S., Tennyson J., Waldmann I.P. *Astron. Astrophys*., **605**, A95 (2017).
36. Rey M., Nikitin A.V., Tyuterev V.G. *Astrophys. J*., **847** (2), aa8909 (2017).
37. Dubernet M.-L., Antony B.K., Ba Y.A., et al. *J. Phys. B. At. Mol. Opt. Phys*., **49** (7), 074003 (2016).
38. Sharpe S.W., Johnson T.J., Sams R.L., et al. *Appl. Spectrosc*., **58** (12), 1452 (2004).
39. https://nwir.pnl.gov/nsd/NSD.nsf/welcome.
40. https://kinetics.kaust.edu.sa/Documents/Methane%20FTIR%20Data-296K.txt.
41. Et-touhami Es-sebbar, Farooq A. *J. Quant. Spectrosc. Radiat. Transfer*, **149**, 241 (2014).
42. Tonkov M.V. *Sorosovskii Obrazovat. Zh.*, **7** (1), 82 (2001).
43. Voitsekhovskaya O.K., Egorov O.V., Kashirskii D.E. *Russ. Phys. J.*, **60** (2), 261 (2017) [*Izv. Vyssh. Uchebn. Zaved., Ser. Fiz.*, **60** (2), 57 (2017)].
44. Voitsekhovskaya O.K., Kashirskii D.E., Korchikov V.S. *Moscow Univ. Phys. Bull.*, **65** (5), 386 (2010) [*Vestn. Moskovsk. Univ., Ser. Fiz., Astronom.*, (5), 50 (2010)].
45. Basov N.G., Hager G.D., Ionin A.A., et al. *IEEE J. Quantum Electron*., **36** (7), 810 (2000).
46. Ionin A.A., Klimachev Yu.M., Kozlov A.Yu., et al. *J. Appl. Spectrosc.*, **81** (2), 309 (2014) [*Zh. Prikl. Spektrosk.*, **81** (2), 313 (2014)].
47. Ionin A.A., Klimachev Yu.M., Kozlov A.Yu., et al. *Atmos. Ocean. Opt.*, **26** (1) 68 (2013) [*Opt. Atmos. Okeana*, **25** (8), 702 (2012)].
48. Airapetyan V.S. *Vestn. Novosibirsk. Gos. Univer., Ser. Fiz.*, **4** (3), 25 (2009).
49. Prabhakara C., Fraser R.S., Dalu G., et al. *J. Appl. Meteorol*., **27**, 379 (1988).
50. Yang P., Wendish M., Bi L. *J. Quant. Spectrosc. Radiat. Transfer*, **112**, 2035 (2011).
51. Shefer O.V. *J. Quant. Spectrosc. Radiat. Transfer*, **201**, 148 (2017).
52. Shefer O.V. *J. Quant. Spectrosc. Radiat. Transfer*, **178**, 350 (2016).
53. Gao M., Yang P., Kattawar G.W. *J. Quant. Spectrosc. Radiat. Transfer*, **131**, 72 (2013).